

Energy levels, radiative rates and electron impact excitation rates for transitions in Fe XIV

Kanti M. Aggarwal^{1*} and Francis P. Keenan¹

¹*Astrophysics Research Centre, School of Mathematics and Physics, Queen's University Belfast, Belfast BT7 1NN, Northern Ireland, UK*

Accepted 2014 September 11. Received 2014 September 11; in original form 2014 July 18

ABSTRACT

Energies and lifetimes are reported for the lowest 136 levels of Fe XIV, belonging to the $(1s^2 2s^2 2p^6) 3s^2 3p, 3s 3p^2, 3s^2 3d, 3p^3, 3s 3p 3d, 3p^2 3d, 3s 3d^2, 3p 3d^2$ and $3s^2 4\ell$ configurations. Additionally, radiative rates, oscillator strengths and line strengths are calculated for all electric dipole (E1), magnetic dipole (M1), electric quadrupole (E2) and magnetic quadrupole (M2) transitions. Theoretical lifetimes determined from these radiative rates for most levels show satisfactory agreement with earlier calculations, as well as with measurements. Electron impact excitation collision strengths are also calculated with the Dirac atomic R -matrix code (DARC) over a wide energy range up to 260 Ryd. Furthermore, resonances have been resolved in a fine energy mesh to determine effective collision strengths, obtained after integrating the collision strengths over a Maxwellian distribution of electron velocities. Results are listed for all 9180 transitions among the 136 levels over a wide range of electron temperatures, up to $10^{7.1}$ K. Comparisons are made with available results in the literature, and the accuracy of the present data is assessed.

Key words: atomic data – atomic processes

1 INTRODUCTION

Iron is an abundant element in solar and other astrophysical plasmas, and its emission lines are detected in all ionization stages. To analyse the vast amount of observational data available from space missions such as SOHO, *Chandra*, XMM-*Newton* and *Hinode*, theoretical atomic data for Fe ions are required, as there generally is paucity of experimental results.

Emission lines of Fe XIV have been widely observed in a variety of solar and other astrophysical plasmas, and over a wide wavelength range from the optical to extreme ultra-violet – see, for example, Jupén et al. (1993), Thomas & Neupert (1994), Lamzin et al. (2001) and Brown et al. (2008). The strongest observed solar forbidden transition is from the coronal green line $(3s^2 3p) \ ^2P_{1/2}^o - \ ^2P_{3/2}^o$ at a wavelength of 5303 Å. This emission line has been widely used for the study of the electron density distribution in the solar corona (Fisher 1978) as well as for coronal oscillations in connection with coronal heating and energy transport (Dermendjiev et al. 1992). Many of the Fe XIV line pairs are density and/or temperature sensitive, and hence provide useful information about physical conditions of the plasmas (see for

example, Bhatia et al. (1994), Brosius et al. (1998) and references therein). However, to reliably analyse observations, atomic data are required for many parameters, including energy levels, radiative rates (A-values) and excitation rates. Since experimental data are generally not available, except for energy levels, theoretical results are required.

Considering the importance of Fe XIV, particularly as a solar plasma diagnostic, many calculations have been performed in the past, particularly for energy levels and A-values, such as those by Huang (1989), Storey, Mason & Saraph (1996), Storey, Mason & Young (2000), Safronova et al. (2002), Gupta & Msezane (2001, 2005), Froese-Fischer, Tachiev & Irimia (2006), Dong et al. (2006) and Wei et al. (2008). However, most of these calculations are confined to transitions among the lowest 40 levels of the $n = 3$ configurations, although Gupta & Msezane and Wei et al. have also included some levels of the $n = 4$ configurations. Similarly, Tayal (2008) has published energy levels, radiative rates and effective collision strengths for some transitions among the lowest 59 levels of the $(1s^2 2s^2 2p^6) 3s^2 3p, 3s 3p^2, 3s^2 3d, 3p^3, 3s 3p 3d$ and $3p^2 3d$ configurations of Fe XIV. However, in a more recent paper, Liang et al. (2010) have reported A-values for a larger number of transitions among 197 levels of Fe XIV. Nevertheless, most of these workers have reported A-values for the electric dipole (E1) transitions alone, whereas in the modelling of plasmas the corresponding results are

* E-mail: K.Aggarwal@qub.ac.uk(KMA); F.Keenan@qub.ac.uk (FPK)

also required for other types of transitions, namely electric quadrupole (E2), magnetic dipole (M1) and magnetic quadrupole (M2). Therefore, the aim of the present work is to extend the earlier available calculations, and to report a complete set of results for all transitions, which can be confidently applied in plasma modelling.

Corresponding calculations for electron impact excitation of Fe XIV are comparatively fewer, and the most notable ones are those by Dufton & Kingston (1991), Storey et al. (1996, 2000), Tayal (2008) and Liang et al. (2010). Most of the earlier calculations for collision strengths (Ω), or more appropriately effective collision strengths (Υ), provided conflicting estimates for the physical parameters of the plasmas – see, for example, Ferguson et al. (1997). Similarly, there was a large scatter between the ratios of observed and predicted intensities for many emission lines of Fe XIV, which varied between 0.23 and 6.20, as discussed and demonstrated by Brickhouse, Raymond & Smith (1995). Some of the discrepancies noted by Brickhouse et al. and Young, Landi & Thomas (1998) were later resolved by Storey et al. (2000), who also performed a large collisional calculation among the lowest 40 levels of the $3s^23p$, $3s3p^2$, $3s^23d$, $3p^3$ and $3s3p3d$ configurations. For the determination of energy levels and radiative rates, they adopted the *SuperStructure* (SS) code of Eissner, Jones & Nussbaumer (1974), and for the scattering process the *R*-matrix code of Berrington et al. (1978) was used. The calculations were basically performed in the *LS* coupling (Russell-Saunders or spin-orbit coupling), but mass and Darwin relativistic energy shifts were included through the *term coupling coefficients* while transforming the *LS* coupling reactance matrices to the intermediate coupling scheme. They calculated values of Ω up to an energy of 100 Ryd, and resolved resonances in a fine energy mesh in the thresholds region. Furthermore, they reported values of effective collision strengths (Υ) over a wide range of electron temperatures up to $10^{7.2}$ K, but only for transitions from the lowest two levels to the excited levels of the $3s3p^2$ and $3s^23d$ configurations. Therefore, their results are too limited for a full and complete application to plasma modelling. In addition, their range of partial waves ($L \leq 18$) is generally insufficient to obtain converged values of Ω , although they included the contribution of higher neglected partial waves through a top-up. Similarly, the energy range of their calculations is insufficient to provide converged values of Υ up to $T_e = 10^{7.2}$ K, although it may not affect the limited set of transitions for which they reported results.

The limitations of Storey et al. (2000) calculations were addressed by Tayal (2008), who included 135 levels of the $3s^23p$, $3s3p^2$, $3s^23d$, $3p^3$, $3s3p3d$, $3p^23d$, $3s3d^2$, $3p3d^2$, $3s^24s$, $3s^24p$ and $3s^24d$ configurations. For the calculation of energy levels and the *A*-values, he adopted the multi-configuration Hartree-Fock (MCHF) codes of Froese-Fischer (1991) and Zatsarinny & Froese-Fischer (1999), while for the scattering process the semi-relativistic *R*-matrix code of Berrington, Eissner & Norrington (1995) was used. Furthermore, he calculated values of Ω up to an energy of 150 Ryd, although the range of partial waves adopted ($J \leq 25$) is insufficient at higher energies, for the convergence of the allowed and some of the forbidden transitions. However, he included the contribution of higher neglected partial waves through a top-up, as also undertaken by Storey et al. Similarly, he resolved resonances in the thresholds region and calculated values

of Υ up to $T_e = 10^7$ K. Therefore, his calculations should provide a clear improvement over those of Storey et al. Unfortunately, as noted above, he reported values of Υ for only some transitions among the lowest 59 levels, and hence are not fully sufficient for plasma modelling where a complete set of data are desirable (Del Zanna, Berrington & Mason 2004).

The limitation in the Tayal (2008) results was removed by Liang et al. (2010), who not only performed a larger calculation among 197 levels of the $3s^23p$, $3s3p^2$, $3s^23d$, $3p^3$, $3s3p3d$, $3p^23d$, $3s3d^2$, $3p3d^2$, $3s^24l$, $3s3p4s$, $3s3p4p$ and $3s3p4d$ configurations, but also reported results of Υ for all transitions among these levels. To determine the atomic structure they adopted the *AutoStructure* (AS) code of Badnell (1997), and for collisional data the *R*-matrix code of Berrington et al. (1995). Similar to the calculations of Storey et al. (2000), their Ω were primarily generated in *LS* coupling and corresponding results for *fine-structure* transitions obtained through their intermediate coupling frame transformation (ICFT) method. However, they included a larger range of partial waves (up to $J = 41$), resolved resonances in a fine mesh of energy (~ 0.0017 Ryd), and reported values of Υ up to a very high temperature of $\sim 4 \times 10^8$ K. Nevertheless, they left some scope for improvement. For example, they included electron exchange only up to $J = 12$, and for $J \geq 13$ adopted a coarse mesh of energy of ~ 0.34 Ryd. More importantly, they performed calculations of Ω in a limited range of energy (~ 90 Ryd), insufficient for the accurate determination of Υ up to $T_e = 4 \times 10^8$ K (~ 2533 Ryd), although they did take into account the high energy expansion of Ω , based on the formulations suggested by Burgess & Tully (1992). Such compromises in the calculations may explain the large discrepancies in Υ noted by them with previous work. For a large number of transitions and at all temperatures, the Liang et al. (2010) results are significantly higher than those of Storey et al. (2000) and Tayal (2008) – see their fig. 4. Given the importance of Fe XIV in astrophysics, we have therefore performed yet another calculation using a completely different approach.

For the generation of wavefunctions we have adopted the GRASP (general-purpose relativistic atomic structure package) code, originally developed by Grant et al. (1980) but revised by Dr. P. H. Norrington. It is a fully relativistic code, based on the *jj* coupling scheme, available at the website <http://web.am.qub.ac.uk/DARC/>, and has been successfully applied by us (and other workers) to a wide range of ions. Further relativistic corrections arising from the Breit interaction and QED effects have also been included. Additionally, we have used the option of *extended average level* (EAL), in which a weighted (proportional to $2j+1$) trace of the Hamiltonian matrix is minimized. This produces a compromise set of orbitals describing closely lying states with moderate accuracy. For the scattering calculations, the *Dirac atomic R-matrix code* (DARC) of P. H. Norrington and I. P. Grant has been adopted. This is a relativistic version of the standard *R*-matrix code, is based on the *jj* coupling scheme, and hence includes fine-structure in the definition of channel coupling. Subsequently, the size of the Hamiltonian matrix increases in a calculation, but it (generally) leads to higher accuracy (for Ω and subsequently

Table 1. Energy levels (in Ryd) of Fe XIV and lifetimes (s). ($a\pm b \equiv a \times 10^{\pm b}$).

Index	Configuration/Level	NIST	GRASP1a	GRASP1b	GRASP2	SST	ICFT	τ (s)
1	3s ² 3p 2P _{1/2} ^o	0.00000	0.00000	0.00000	0.00000	0.00000	0.00000
2	3s ² 3p 2P _{3/2} ^o	0.17180	0.17535	0.17074	0.17067	0.16239	0.16705	1.692-02
3	3s3p ² 4P _{1/2}	2.05139	2.03234	2.03064	2.02900	2.03507	2.01971	3.139-08
4	3s3p ² 4P _{3/2}	2.12133	2.10370	2.09992	2.09815	2.08944	2.08747	1.675-07
5	3s3p ² 4P _{5/2}	2.20879	2.19432	2.18761	2.18561	2.18005	2.17442	4.429-08
6	3s3p ² 2D _{3/2}	2.72689	2.74298	2.73751	2.73105	2.72869	2.71977	4.145-10
7	3s3p ² 2D _{5/2}	2.74719	2.76419	2.75717	2.75061	2.73363	2.73919	5.269-10
8	3s3p ² 2S _{1/2}	3.32333	3.37779	3.37470	3.37569	3.32764	3.34992	5.101-11
9	3s3p ² 2P _{1/2}	3.54036	3.60640	3.60098	3.60187	3.53864	3.57266	2.673-11
10	3s3p ² 2P _{3/2}	3.61328	3.68359	3.67667	3.67745	3.64645	3.64739	2.295-11
11	3s ² 3d 2D _{3/2}	4.31233	4.40724	4.39829	4.36965	4.34655	4.37626	2.133-11
12	3s ² 3d 2D _{5/2}	4.33036	4.42619	4.41499	4.38642	4.36841	4.39805	2.341-11
13	3p ³ 2D _{3/2} ^o	5.25239	5.26092	5.25358	5.25271	5.25299	5.23628	2.147-10
14	3p ³ 2D _{5/2} ^o	5.28747	5.29554	5.28593	5.28494	5.26203	5.26904	2.548-10
15	3p ³ 4S _{3/2} ^o	5.36738	5.39484	5.38808	5.38792	5.37027	5.36191	2.715-11
16	3s3p(3P)3d 4F _{3/2} ^o		5.86121	5.85238	5.85283	5.85599	5.85344	2.872-09
17	3s3p(3P)3d 4F _{5/2} ^o	5.88668	5.89986	5.88910	5.88950	5.89250	5.89074	3.185-09
18	3p ³ 2P _{1/2} ^o	5.85316	5.90425	5.89621	5.89598	5.85859	5.86547	5.830-11
19	3p ³ 2P _{3/2} ^o	5.88140	5.93513	5.92504	5.92464	5.88606	5.89391	5.910-11
20	3s3p(3P)3d 4F _{7/2} ^o	5.94097	5.95608	5.94279	5.94310	5.94483	5.94453	3.547-09
21	3s3p(3P)3d 4F _{9/2} ^o	6.01676	6.03421	6.01785	6.01804	6.01696	6.01885	1.927-02
22	3s3p(3P)3d 4P _{5/2} ^o	6.29051	6.32562	6.31451	6.31655	6.31608	6.31613	3.335-11
23	3s3p(3P)3d 4D _{3/2} ^o	6.31200	6.34978	6.33917	6.34120	6.33546	6.33640	2.734-11
24	3s3p(3P)3d 4D _{1/2} ^o	6.32572	6.36637	6.35636	6.35842	6.34811	6.35006	2.328-11
25	3s3p(3P)3d 4P _{1/2} ^o	6.41304	6.44657	6.43439	6.43625	6.42631	6.42949	3.300-11
26	3s3p(3P)3d 4P _{3/2} ^o	6.41722	6.45447	6.44143	6.44333	6.43210	6.43638	2.838-11
27	3s3p(3P)3d 4D _{7/2} ^o	6.40979	6.45542	6.44028	6.44219	6.43175	6.43704	2.318-11
28	3s3p(3P)3d 4D _{5/2} ^o	6.41636	6.45847	6.44464	6.44657	6.43433	6.43956	2.502-11
29	3s3p(3P)3d 2D _{3/2} ^o	6.53556	6.59908	6.58702	6.59017	6.56402	6.57354	2.629-11
30	3s3p(3P)3d 2D _{5/2} ^o	6.54163	6.60483	6.59156	6.59466	6.56984	6.57957	2.700-11
31	3s3p(3P)3d 2F _{5/2} ^o	6.78862	6.88364	6.87251	6.87715	6.84338	6.84840	5.516-11
32	3s3p(3P)3d 2F _{7/2} ^o	6.92393	7.02305	7.00797	7.01246	6.97121	6.98042	5.175-11
33	3s3p(3P)3d 2P _{3/2} ^o	7.35495	7.48700	7.47685	7.48278	7.40442	7.44321	1.820-11
34	3s3p(3P)3d 2P _{1/2} ^o		7.56294	7.55022	7.55569	7.47391	7.51553	2.024-11
35	3s3p(1P)3d 2F _{7/2} ^o	7.45046	7.58427	7.57027	7.57062	7.53250	7.54744	1.823-11
36	3s3p(1P)3d 2F _{5/2} ^o	7.47787	7.61169	7.59845	7.59883	7.55632	7.57198	1.771-11
37	3s3p(1P)3d 2P _{1/2} ^o	7.65001	7.81047	7.79952	7.80479	7.70946	7.74820	1.422-11
38	3s3p(1P)3d 2D _{3/2} ^o	7.66171	7.82117	7.80858	7.81542	7.75141	7.76494	1.311-11
39	3s3p(1P)3d 2P _{3/2} ^o	7.68796	7.84847	7.83550	7.84181	7.72717	7.78882	1.341-11
40	3s3p(1P)3d 2D _{5/2} ^o	7.69544	7.85291	7.83914	7.84730	7.76433	7.79871	1.185-11
41	3p ² (1D)3d 2F _{5/2}		8.79290	8.77901	8.77181	8.76349	8.76535	1.520-10
42	3p ² (1D)3d 2F _{7/2}		8.85638	8.83992	8.83356	8.82680	8.82720	1.286-10
43	3p ² (3P)3d 4F _{3/2}		8.87136	8.86119	8.83652	8.81852	8.82377	5.523-11
44	3p ² (3P)3d 4F _{5/2}	8.84793	8.91446	8.90219	8.87824	8.86051	8.86553	5.467-11
45	3p ² (3P)3d 4F _{7/2}	8.90566	8.97278	8.95785	8.93461	8.91954	8.92177	5.394-11
46	3p ² (3P)3d 2P _{3/2}		9.01893	9.00611	9.00385	8.98134	8.98871	3.985-11
47	3p ² (3P)3d 4F _{9/2}	8.96590	9.03865	9.02061	8.99543	8.99559	8.98318	5.401-11
48	3p ² (3P)3d 4D _{1/2}		9.06018	9.04870	9.04527	9.01874	9.02674	4.297-11
49	3p ² (3P)3d 4D _{3/2}	9.07430	9.13000	9.11570	9.11085	9.08454	9.09281	4.257-11
50	3p ² (3P)3d 4D _{5/2}	9.07876	9.13814	9.12319	9.11668	9.08990	9.09892	4.452-11
51	3p ² (3P)3d 2P _{1/2}		9.19927	9.18174	9.17963	9.15468	9.16113	3.761-11
52	3p ² (3P)3d 4D _{7/2}	9.14126	9.20148	9.18329	9.17746	9.15059	9.15923	4.566-11
53	3p ² (1D)3d 2G _{7/2}		9.37083	9.35533	9.31571	9.27154	9.29897	1.430-10
54	3p ² (1D)3d 2G _{9/2}		9.40888	9.39048	9.35153	9.29434	9.33577	1.435-10
55	3p ² (1D)3d 2D _{5/2}	9.41158	9.54495	9.53033	9.48587	9.45564	9.46853	1.803-11
56	3p ² (1D)3d 2D _{3/2}	9.44965	9.57682	9.56272	9.51950	9.48529	9.49919	1.899-11
57	3p ² (3P)3d 4P _{5/2}	9.51938	9.65260	9.63568	9.59352	9.55827	9.57017	1.544-11
58	3p ² (3P)3d 4P _{1/2}	9.51534	9.65716	9.64323	9.59977	9.55699	9.56728	1.298-11

Table 1. Energy levels (in Ryd) of Fe XIV and lifetimes (s). ($a \pm b \equiv a \times 10^{\pm b}$).

Index	Configuration/Level	NIST	GRASP1a	GRASP1b	GRASP2	SST	ICFT	τ (s)
59	$3p^2(^3P)3d$ $^4P_{3/2}$	9.52301	9.65785	9.64277	9.59996	9.56065	9.57123	1.401-11
60	$3p^2(^1D)3d$ $^2P_{1/2}$		9.94094	9.92656	9.91499	9.84485	9.87842	2.345-11
61	$3p^2(^1D)3d$ $^2P_{3/2}$		9.96981	9.95549	9.93515	9.85545	9.89434	2.691-11
62	$3p^2(^1D)3d$ $^2S_{1/2}$		10.04211	10.02659	10.02387	9.96081	9.99112	2.231-11
63	$3p^2(^1S)3d$ $^2D_{3/2}$	9.99024	10.08319	10.06836	10.03172	9.94919	9.98623	2.916-11
64	$3p^2(^1S)3d$ $^2D_{5/2}$		10.18284	10.16632	10.10569	10.02262	10.06287	3.182-11
65	$3p^2(^3P)3d$ $^2F_{5/2}$	10.02380	10.21222	10.19747	10.14776	10.07283	10.11260	1.475-11
66	$3p^2(^3P)3d$ $^2F_{7/2}$	10.06952	10.26216	10.24480	10.18924	10.11673	10.15905	1.410-11
67	$3s3d^2(^3F)$ $^4F_{3/2}$		10.33307	10.31496	10.31070	10.31047	10.31372	1.777-11
68	$3s3d^2(^3F)$ $^4F_{5/2}$		10.34146	10.32214	10.31785	10.31912	10.32265	1.805-11
69	$3s3d^2(^3F)$ $^4F_{7/2}$	10.26393	10.35302	10.33200	10.32766	10.33112	10.33504	1.846-11
70	$3s3d^2(^3F)$ $^4F_{9/2}$		10.36761	10.34435	10.34009	10.34640	10.35077	1.903-11
71	$3s3d^2(^3P)$ $^4P_{1/2}$		10.65477	10.63624	10.63790	10.61843	10.63813	1.422-11
72	$3s3d^2(^3P)$ $^4P_{3/2}$		10.65971	10.64063	10.64230	10.62345	10.64372	1.438-11
73	$3s3d^2(^3P)$ $^4P_{5/2}$		10.66748	10.64640	10.64789	10.61705	10.65235	1.461-11
74	$3p^2(^3P)3d$ $^2D_{5/2}$	10.49750	10.82745	10.81230	10.65921	10.55669	10.61062	1.183-11
75	$3p^2(^3P)3d$ $^2D_{3/2}$		10.87735	10.86186	10.70049	10.60227	10.65415	1.183-11
76	$3s3d^2(^1D)$ $^2D_{5/2}$		11.15225	11.13296	11.08355	10.99852	11.05061	1.233-11
77	$3s3d^2(^1D)$ $^2D_{3/2}$		11.15820	11.13972	11.08552	10.99758	11.05003	1.217-11
78	$3s3d^2(^1G)$ $^2G_{7/2}$	10.93356	11.16290	11.14259	11.07693	11.01250	11.05886	2.220-11
79	$3s3d^2(^1G)$ $^2G_{9/2}$	10.93589	11.16671	11.14541	11.07945	11.01432	11.06128	2.178-11
80	$3s3d^2(^3F)$ $^2F_{5/2}$	11.33444	11.62829	11.61037	11.54361	11.42111	11.48263	1.084-11
81	$3s3d^2(^3F)$ $^2F_{7/2}$	11.34596	11.63928	11.61899	11.55422	11.43580	11.49754	1.118-11
82	$3s3d^2(^1S)$ $^2S_{1/2}$		11.85406	11.83668	11.82613	11.68813	11.76614	9.918-12
83	$3s3d^2(^3p)$ $^2P_{1/2}$		12.02187	12.00516	11.86971	11.71686	11.79288	8.195-12
84	$3s3d^2(^3P)$ $^2P_{3/2}$		12.04117	12.02267	11.88339	11.72474	11.79945	8.262-12
85	$3p3d^2(^3F)$ $^4G_{5/2}^o$		12.48449	12.46645	12.46736	12.45928	12.46422	6.816-11
86	$3p3d^2(^3P)$ $^4G_{7/2}^o$		12.53096	12.51043	12.51131	12.50063	12.50901	6.733-11
87	$3p3d^2(^3F)$ $^4G_{9/2}^o$		12.59125	12.56760	12.56844	12.55370	12.56670	6.604-11
88	$3p3d^2(^3F)$ $^4G_{11/2}^o$		12.66904	12.64158	12.64235	12.61846	12.64033	6.499-11
89	$3p3d^2(^1D)$ $^2F_{5/2}^o$		12.79348	12.77416	12.77527	12.75199	12.75948	3.854-11
90	$3p3d^2(^3F)$ $^2D_{3/2}^o$		12.86491	12.84510	12.84634	12.83374	12.83546	2.922-11
91	$3p3d^2(^1D)$ $^2F_{7/2}^o$		12.89459	12.87080	12.87197	12.85061	12.85293	3.811-11
92	$3p3d^2(^3F)$ $^2D_{5/2}^o$		12.92026	12.89695	12.89810	12.85678	12.88759	3.225-11
93	$3p3d^2(^3P)$ $^4D_{1/2}^o$		12.97600	12.95762	12.95874	12.94450	12.95819	3.013-11
94	$3p3d^2(^3P)$ $^2S_{1/2}^o$		12.99686	12.97734	12.97870	13.00402	12.98585	1.948-11
95	$3p3d^2(^3P)$ $^4D_{3/2}^o$		13.01803	12.99730	12.99839	12.96792	12.99476	3.124-11
96	$3p3d^2(^3P)$ $^4D_{5/2}^o$		13.06047	13.03778	13.03933	13.00404	13.03206	2.508-11
97	$3p3d^2(^3F)$ $^4F_{3/2}^o$		13.06494	13.04571	13.04864	13.01722	13.03749	1.508-11
98	$3p3d^2(^3F)$ $^4F_{5/2}^o$		13.07361	13.05035	13.05257	13.05402	13.04542	2.064-11
99	$3p3d^2(^3F)$ $^4F_{7/2}^o$		13.08689	13.06545	13.06793	13.03258	13.06110	1.728-11
100	$3p3d^2(^3F)$ $^4F_{9/2}^o$		13.11152	13.08744	13.09003	13.08149	13.07704	1.736-11
101	$3p3d^2(^3P)$ $^4D_{7/2}^o$		13.12848	13.10403	13.10592	13.04618	13.09812	2.138-11
102	$3p3d^2(^1G)$ $^2G_{7/2}^o$		13.18181	13.15906	13.16058	13.09772	13.13120	2.335-11
103	$3p3d^2(^1G)$ $^2G_{9/2}^o$		13.19006	13.16537	13.16715	13.11278	13.14554	2.334-11
104	$3p3d^2(^3P)$ $^4P_{3/2}^o$		13.19304	13.17196	13.17340	13.15374	13.17168	2.380-11
105	$3p3d^2(^3P)$ $^4P_{1/2}^o$		13.20608	13.18390	13.18527	13.12434	13.18468	2.219-11
106	$3s^24s$ $^2S_{1/2}$	13.07686	13.25548	13.24529	13.14370	13.03032	13.08248	4.012-12
107	$3p3d^2(^3P)$ $^4P_{5/2}^o$		13.25717	13.23365	13.23506	13.20334	13.23196	2.346-11
108	$3p3d^2(^1G)$ $^2H_{9/2}^o$		13.36974	13.34587	13.34706	13.30292	4.631-11
109	$3p3d^2(^3F)$ $^4D_{7/2}^o$		13.42736	13.40323	13.40707	13.35810	13.39085	1.218-11
110	$3p3d^2(^3F)$ $^4D_{5/2}^o$		13.43131	13.40871	13.41268	13.35696	13.39153	1.200-11
111	$3p3d^2(^3F)$ $^4D_{3/2}^o$		13.43361	13.41236	13.41637	13.36196	13.39113	1.180-11
112	$3p3d^2(^3F)$ $^4D_{1/2}^o$		13.43819	13.41725	13.42128	13.36664	13.39412	1.173-11
113	$3p3d^2(^1G)$ $^2H_{11/2}^o$		13.47291	13.44681	13.44787	13.39731	5.240-11
114	$3p3d^2(^1D)$ $^2P_{3/2}^o$		13.54657	13.52522	13.52710	13.47998	13.50738	1.220-11
115	$3p3d^2(^1D)$ $^2P_{1/2}^o$		13.61203	13.58880	13.58929	13.53450	13.57282	1.248-11
116	$3p3d^2(^3P)$ $^4S_{3/2}^o$		13.76928	13.74736	13.75183	13.66053	13.70923	7.871-12

Table 1. Energy levels (in Ryd) of Fe XIV and lifetimes (s). ($a\pm b \equiv a \times 10^{\pm b}$).

Index	Configuration/Level	NIST	GRASP1a	GRASP1b	GRASP2	SST	ICFT	τ (s)
117	3p3d ² (³ F) ² F _{5/2} ^o		13.83318	13.81117	13.81521	13.73004	13.76007	1.509-11
118	3p3d ² (¹ G) ² F _{7/2} ^o		13.85692	13.83338	13.83695	13.73955	13.78209	1.719-11
119	3p3d ² (¹ D) ² D _{3/2} ^o		13.98712	13.96663	13.97205	13.85764	13.91184	1.121-11
120	3p3d ² (¹ D) ² D _{5/2} ^o		14.04146	14.01795	14.02364	13.90501	13.96299	1.123-11
121	3p3d ² (¹ S) ² P _{1/2} ^o		14.04675	14.02866	14.02414	13.94378	13.98707	2.264-11
122	3p3d ² (¹ S) ² P _{3/2} ^o		14.16445	14.14214	14.13714	14.04766	14.09894	2.233-11
123	3p3d ² (³ F) ² F _{7/2} ^o		14.24202	14.22046	14.22687	14.08701	14.12216	1.305-11
124	3p3d ² (¹ G) ² F _{5/2} ^o		14.30263	14.27985	14.28582	14.12242	14.18067	1.396-11
125	3s ² 4p ² P _{1/2} ^o	14.29632	14.31291	14.30321	14.18731	14.13387	14.07465	1.743-11
126	3p3d ² (³ F) ² G _{9/2} ^o		14.35240	14.32774	14.33480	14.15420	14.21792	1.266-11
127	3s ² 4p ² P _{3/2} ^o	14.34343	14.37783	14.36636	14.24844	14.18940	14.14366	1.802-11
128	3p3d ² (³ F) ² G _{7/2} ^o		14.38156	14.35734	14.36431	14.16256	14.24911	1.281-11
129	3p3d ² (³ P) ² D _{5/2} ^o		14.71748	14.69503	14.70360	14.50304	14.57380	9.667-12
130	3p3d ² (³ P) ² D _{3/2} ^o		14.72401	14.70309	14.71140	14.51296	14.57864	9.465-12
131	3p3d ² (³ P) ² P _{1/2} ^o		14.92128	14.90027	14.89664	14.68134	14.76515	7.765-12
132	3p3d ² (³ P) ² P _{3/2} ^o		14.93990	14.91830	14.91445	14.69930	14.78444	7.704-12
133	3s ² 4d ² D _{3/2}	15.45491	15.72443	15.71151	15.61108	15.48934	15.49803	3.455-12
134	3s ² 4d ² D _{5/2}	15.46684	15.73484	15.72089	15.62151	15.50092	15.51137	3.412-12
135	3s ² 4f ² F _{5/2} ^o	16.29929	16.53545	16.52042	16.47274	16.35952	1.211-12
136	3s ² 4f ² F _{7/2} ^o	16.29692	16.53847	16.52331	16.47576	16.36331	1.214-12

NIST: <http://www.nist.gov/pml/data/asd.cfm>

GRASP1a: Energies from the GRASP code with 136 level calculations without Breit and QED effects

GRASP1b: Energies from the GRASP code with 136 level calculations with Breit and QED effects

GRASP2: Energies from the GRASP code with 332 level calculations with Breit and QED effects

SST: Energies of Tayal (2008) from the MCHF code

ICFT: Energies of Liang et al. (2010) from the AS code

Υ), especially for transitions among the *fine-structure* levels of a state, because resonances through the energies of degenerating levels are also taken into account. Since degeneracy among some of the levels is significant, see for example the $3s3p(^3P)3d^4F_{3/2,5/2,7/2,9/2}^o$ levels in Table 1, the use of this code, we believe, is more appropriate. It is unpublished but is freely available at the website <http://web.am.qub.ac.uk/DARC/>, and has been successfully applied by us and other users to a wide range of ions.

2 ENERGY LEVELS

The $(1s^22s^22p^6) 3s^23p, 3s3p^2, 3s^23d, 3p^3, 3s3p3d, 3p^23d, 3s3d^2, 3p3d^2$ and $3s^24\ell$ configurations of Fe XIV give rise to the lowest 136 levels listed in Table 1, where we compare our energies with the experimental values compiled by the NIST (National Institute of Standards and Technology) team (Kramida et al. 2013), available at their website <http://www.nist.gov/pml/data/asd.cfm>. Energy levels obtained without (GRASP1a) and with (GRASP1b) the Breit and QED corrections are included in the Table. The inclusion of Breit and QED effects has (in general) lowered the energies by a maximum of 0.03 Ryd, i.e. $\leq 0.3\%$. Additionally, their inclusion has altered the orderings in a few instances, such as for levels 26/27, 58/59 and 106/107. The energy differences for these swapped levels are very small and we have retained the original orderings because subsequent tables for A- and Υ values follow these. However, the effect of these corrections is significant for the $3s^23p^2P_{3/2}^o$ level (2), where the energy has become lower by 0.00461 Ryd, i.e. 2.6%. As a result, there is now a better match for this level with the experimental energy of NIST. For a majority of levels, there is good agreement between our calculations and the experimental values, both in magnitude and orderings. Differences, if any, are within 0.3 Ryd – see levels 37-40 or 78-81. Similarly, there are some minor differences in the level orderings, but the most notable is level 18 ($3p^3^2P_{1/2}^o$).

The differences between our energy levels from GRASP and those of Tayal (2008) are up to 0.3 Ryd (1.5%) for a few levels, such as 82-84 and 126-132. Furthermore, the level orderings of Tayal do not match in a few cases with our calculations or the experimental results – see, for example, levels 38/39. More importantly, his energy for level 2 ($3s^23p^2P_{3/2}^o$) is lower than the experimental or any other theoretical value listed in Table 1, by up to 5%. This is in spite of the fact that he adopted non-orthogonal orbitals and hence optimised each state separately and independently, a procedure that generally yields better agreement between theory and measurement. However, we note here that although this level is very important as stated in section 1, a difference of 5% is not uncommon among Fe XIV calculations – see, for example, table 4 of Wei et al. (2008). Our calculated energies are based only on spectroscopic levels, but can be improved with additional CI or the inclusion of pseudo-orbitals. However, this is not possible bearing in mind our further calculations for other important parameters, particularly the collision strengths. For this reason, the accuracy of the energy levels (wave functions) included in the collisional calculation by Tayal is lower by $\sim 1\%$ than those listed in Table 1, because

he deleted all those configurations with coefficients less than 0.02 in magnitude.

Liang et al. (2010) adopted the *AutoStructure* (AS) code of Badnell (1997) to calculate energies for 197 levels of Fe XIV. The 61 levels in addition to our calculation have arisen from the $3d^3$ and $3s3p4s/4p/4d$ configurations. In fact, these four configurations give rise to 67 levels, but they omitted 6 from $3s3p4d$. However, to improve the accuracy they included further CI with additional 77 configurations, namely $3s3p4f, 3p^24\ell, 3p3d4\ell, 3d^24\ell, 3\ell4\ell4\ell'$ and $3\ell3\ell'5\ell$. As a result, their calculated energies are expected to be more accurate and are included in Table 1 for comparison. Differences with the NIST compilations are generally smaller, but are up to 1.4% for some levels, such as $3s^24p^2P_{1/2,3/2}^o$, for which our GRASP1b energies agree better with the measurements. Similarly, their calculated energy for the $3s^23p^2P_{3/2}^o$ level (2) is lower than the experimental value by $\sim 3\%$, only slightly improving over the Tayal (2008) result. Nevertheless, differences with our calculated (GRASP1b) energies are up to 0.2 Ryd for some of the levels, such as $3s^24p^2P_{1/2,3/2}^o$, as noted above.

To assess the effect of additional CI, we have also performed a larger calculation (GRASP2) with 332 levels, which arise from the $3s^23p, 3s3p^2, 3s^23d, 3p^3, 3s3p3d, 3p^23d, 3s3d^2, 3p3d^2, 3d^3, 3s^24\ell, 3s3p4\ell, 3s^25\ell$ and $3s3p5\ell$ configurations. Almost all the additional 196 levels of the $3d^3, 3s3p4\ell, 3s^25\ell$ and $3s3p5\ell$ configurations yield energies *above* those of the 136 included in GRASP1 and listed in Table 1. Hence their inclusion in a collisional calculation may improve the accuracy of Υ , because of the additional resonances arising from these levels, but the effect on the energies of lower levels will not be significant, because there is no intermixing among the levels. This is confirmed by the comparison shown in Table 1 as most of the levels agree within 0.05 Ryd and the orderings are also nearly the same. However, for some of the levels the differences between the GRASP1 and GRASP2 energies are up to 0.15 Ryd – see for example, levels 74/75, 83/84 and 125/127. In some cases the energies obtained in GRASP2 have become better (i.e. are closer to those of NIST) but are worse for others, such as 125/127, i.e. $3s^24p^2P_{1/2,3/2}^o$. Therefore, there is no overall advantage of extensive CI for the determination of energy levels for Fe XIV. Finally, based on the comparisons shown in Table 1 and discussed henceforth we may conclude that our calculated energy levels are accurate to about 1%.

3 RADIATIVE RATES

The absorption oscillator strength (f_{ij}) and radiative rate A_{ji} (in s^{-1}) for a transition $i \rightarrow j$ are related by the following expression:

$$f_{ij} = \frac{mc}{8\pi^2 e^2} \lambda_{ji}^2 \frac{\omega_j}{\omega_i} A_{ji} = 1.49 \times 10^{-16} \lambda_{ji}^2 \frac{\omega_j}{\omega_i} A_{ji} \quad (1)$$

where m and e are the electron mass and charge, respectively, c is the velocity of light, λ_{ji} is the transition energy/wavelength in \AA , and ω_i and ω_j are the statistical weights of the lower (i) and upper (j) levels, respectively. Similarly, the oscillator strength f_{ij} (dimensionless) and the line strength S (in atomic unit) are related by the standard equations listed below.

Table 2. Transition wavelengths (λ_{ij} in Å), radiative rates (A_{ji} in s^{-1}), oscillator strengths (f_{ij} , dimensionless), and line strengths (S, in atomic units) for electric dipole (E1), and A_{ji} for E2, M1 and M2 transitions in Fe XIV. ($a \pm b \equiv a \times 10^{\pm b}$). (For complete table see Supporting Information.)

i	j	λ_{ij}	A_{ji}^{E1}	f_{ij}^{E1}	S^{E1}	A_{ji}^{E2}	A_{ji}^{M1}	A_{ji}^{M2}
1	2	5.337+03	0.000-00	0.000-00	0.000-00	1.431-02	5.907+01	0.000-00
1	3	4.488+02	2.313+07	6.985-04	2.064-03	0.000-00	0.000-00	0.000-00
1	4	4.340+02	4.779+05	2.698-05	7.710-05	0.000-00	0.000-00	2.089-00
1	5	4.166+02	0.000-00	0.000-00	0.000-00	0.000-00	0.000-00	1.357-00
1	6	3.329+02	2.334+09	7.754-02	1.699-01	0.000-00	0.000-00	1.757-02
1	7	3.305+02	0.000-00	0.000-00	0.000-00	0.000-00	0.000-00	6.144-00
1	8	2.700+02	1.812+10	1.981-01	3.521-01	0.000-00	0.000-00	0.000-00
1	9	2.531+02	1.515+10	1.454-01	2.423-01	0.000-00	0.000-00	0.000-00
1	10	2.479+02	8.171+09	1.505-01	2.456-01	0.000-00	0.000-00	1.785-00
.
.
.

For the electric dipole (E1) transitions

$$A_{ji} = \frac{2.0261 \times 10^{18}}{\omega_j \lambda_{ji}^3} S^{\text{E1}} \quad \text{and} \quad f_{ij} = \frac{303.75}{\lambda_{ji} \omega_i} S^{\text{E1}}, \quad (2)$$

for the magnetic dipole (M1) transitions

$$A_{ji} = \frac{2.6974 \times 10^{13}}{\omega_j \lambda_{ji}^3} S^{\text{M1}} \quad \text{and} \quad f_{ij} = \frac{4.044 \times 10^{-3}}{\lambda_{ji} \omega_i} S^{\text{M1}}, \quad (3)$$

for the electric quadrupole (E2) transitions

$$A_{ji} = \frac{1.1199 \times 10^{18}}{\omega_j \lambda_{ji}^5} S^{\text{E2}} \quad \text{and} \quad f_{ij} = \frac{167.89}{\lambda_{ji}^3 \omega_i} S^{\text{E2}}, \quad (4)$$

and for the magnetic quadrupole (M2) transitions

$$A_{ji} = \frac{1.4910 \times 10^{13}}{\omega_j \lambda_{ji}^5} S^{\text{M2}} \quad \text{and} \quad f_{ij} = \frac{2.236 \times 10^{-3}}{\lambda_{ji}^3 \omega_i} S^{\text{M2}}. \quad (5)$$

In Table 2 we present transition energies/wavelengths (λ , in Å), radiative rates (A_{ji} , in s^{-1}), oscillator strengths (f_{ij} , dimensionless), and line strengths (S, in a.u.), in length form only, for all 2733 electric dipole (E1) transitions among the 136 levels of Fe XIV. The indices used to represent the lower and upper levels of a transition have already been defined in Table 1. Similarly, there are 3776 E2, 2791 M1 and 3643 M2 transitions among the 136 levels. However, only their A- values are listed in Table 2, as this is the quantity required for plasma modelling. The corresponding results for f- and S- values can be easily obtained through the above equations. Furthermore, the S- values have been calculated in both Babushkin and Coulomb gauges, i.e. the length and velocity forms in the widely used non-relativistic nomenclature, but in Table 2 results are listed in the length form alone, because these are generally considered to be comparatively more accurate. Nevertheless, we will discuss later the velocity/length form ratio, as this provides some assessment of the accuracy of the results.

In Table 3 we compare our A- values for some of the E1 transitions, mainly among the lowest 15 levels, from GRASP1 with those of Tayal (2008) and Liang et al. (2010) from the MCHF and AS codes, respectively. Also included in the table are the f- values from our GRASP1 calculations because they are indicative of the strength of a transition. As already stated in section 1, Tayal has not reported A-

values for all transitions, but for the ones in common there are no discrepancies with the corresponding results from our calculations. Similarly, our GRASP1 A- values agree within $\sim 10\%$ with those of Liang et al. for almost all transitions, the only exceptions being a few weak transitions, such as 8–15 ($f \sim 10^{-5}$) and 12–15 ($f \sim 10^{-6}$). This is because weak(er) transitions are more sensitive to mixing coefficients, and hence differing amount of CI (and methods) often produce different f- values, as discussed in detail by Hibbert (2000). However, in general, the f-values for weak(er) transitions are less important in comparison to stronger ones with $f \geq 0.01$, although their inclusion may still be required in modelling applications.

As in the case of the energy levels, the effect of additional CI on the f- (or A-) values is insignificant for a majority of the transitions. This is further confirmed by the A- values from our larger GRASP2 calculations with 332 levels, also listed in Table 3. Therefore, the inclusion of CI is important, but only up to a certain extent, mainly when the levels closely interact among themselves, as also discussed earlier by Aggarwal et al. (2007) for three Mg-like ions. Another useful criterion to assess the accuracy of radiative rates is the ratio (R) of the velocity and length forms of the S- values, included in Table 3. However, such comparisons are only desirable, and are not a fully sufficient test to assess accuracy, as different calculations (or combinations of configurations) may give comparable f- values in the two forms, but entirely different results in magnitude. Generally, the two forms agree satisfactorily for *strong* transitions, but differences can sometimes be substantial even for some very strong transitions, as demonstrated through various examples by Aggarwal et al. (2007). Nevertheless, R is within 0.2 of unity for most (comparatively strong) transitions, and significant departures are for only the weaker ones, such as the last 6 listed in Table 3. Considering all 2733 E1 transitions, R is within 0.2 of unity for most transitions with $f \geq 0.01$, but for 70 ($\sim 2.5\%$) R is up to a factor of 2. For 38 ($\sim 1\%$) weaker transitions, R is over 1000 and examples include 7–92 ($f \sim 10^{-10}$) and 77–111 ($f \sim 10^{-11}$). In conclusion, we may confidently state that for a majority of the strong E1 transitions, our radiative rates are accurate to better than 20%. However, for the weaker transitions this assessment of accuracy does not apply.

Table 3. Comparison of A- values (s^{-1}) for some transitions of Fe XIV. ($a\pm b \equiv a \times 10^{\pm b}$).

Transition		GRASP1		GRASP2	MCHF	AS	R
I	J	A	f	A	A	A	
1	3	2.313+07	6.985-4	2.313+07	2.33+07	2.29+07	8.9-1
1	4	4.779+05	2.698-5	5.133+05	5.68+05	5.06+05	1.2-0
1	6	2.334+09	7.754-2	2.341+09	2.41+09	2.40+09	1.1-0
1	8	1.812+10	1.981-1	1.820+10	1.70+10	1.78+10	9.7-1
1	9	1.515+10	1.454-1	1.511+10	1.49+10	1.49+10	1.0-0
1	10	8.171+09	1.505-1	8.212+09	7.80+09	7.95+09	9.9-1
1	11	3.836+10	4.937-1	3.804+10	3.69+10	3.81+10	1.0-0
2	3	8.724+06	1.570-4	8.788+06	9.16+06	8.88+06	8.1-1
2	4	5.491+06	1.837-4	5.496+06	5.43+06	5.45+06	9.5-1
2	5	2.258+07	1.036-3	2.322+07	2.33+07	2.27+07	1.0-0
2	6	7.886+07	1.490-3	8.179+07	8.79+07	8.82+07	1.2-0
2	7	1.898+09	5.298-2	1.908+09	1.98+09	1.97+09	1.1-0
2	8	1.484+09	8.999-3	1.521+09	1.63+09	1.58+09	8.8-1
2	9	2.226+10	1.177-1	2.231+10	2.14+10	2.19+10	9.7-1
2	10	3.541+10	3.586-1	3.534+10	3.41+10	3.46+10	9.9-1
2	11	8.535+09	5.946-2	8.518+09	8.26+09	8.47+09	1.0-0
2	12	4.272+10	4.428-1	4.239+10	4.15+10	4.27+10	1.0-0
3	13	1.879+08	4.503-3	1.821+08		1.99+08	9.9-1
3	15	6.713+09	1.483-1	6.635+09	6.59+09	6.56+09	9.8-1
4	13	1.312+08	1.642-3	1.269+08		1.47+08	9.9-1
4	14	2.962+06	5.450-5	2.901+06		2.70+06	1.0-0
4	15	1.268+10	1.460-1	1.254+10	1.25+10	1.24+10	9.8-1
5	13	5.092+08	4.496-3	4.957+08		5.44+08	9.5-1
5	14	8.486+07	1.100-3	8.333+07		8.47+07	9.2-1
5	15	1.730+10	1.401-1	1.710+10	1.70+10	1.69+10	9.8-1
6	13	2.151+09	4.230-2	2.098+09	2.23+09	2.20+09	9.4-1
6	14	2.984+08	8.580-3	2.898+08	3.09+08	3.04+08	9.4-1
6	15	7.619+07	1.350-3	7.244+07		8.32+07	8.1-1
7	13	8.838+08	1.177-2	8.615+08	9.00+08	8.94+08	8.2-1
7	14	2.943+09	5.729-2	2.868+09	3.04+09	3.01+09	9.2-1
7	15	9.874+06	1.184-4	1.023+07		1.21+07	1.9-0
8	13	3.161+08	2.229-2	3.063+08		3.20+08	1.1-0
8	15	2.867+05	1.761-5	2.784+05		7.56+04	2.3-0
9	13	4.448+08	4.055-2	4.357+08		4.75+08	1.1-0
9	15	5.653+06	4.407-4	5.218+06		6.51+06	1.4-0
10	13	2.613+07	1.308-3	2.505+07		2.66+07	1.3-0
10	14	5.882+08	4.242-2	5.742+08		6.22+08	1.1-0
10	15	5.494+07	2.335-3	5.400+07		5.65+07	9.4-1
11	13	5.966+06	1.015-3	5.882+06		5.08+06	3.2-1
11	14	3.817+05	9.047-5	3.572+05		3.22+05	2.1-1
11	15	4.099+05	5.209-5	4.297+05		3.90+05	5.0-1
12	13	6.463+05	7.628-5	7.186+05		6.11+05	5.4-1
12	14	6.829+06	1.121-3	6.784+06		5.80+06	3.3-1
12	15	2.627+04	2.302-6	1.293+04		1.12+04	2.3-2

GRASP1: Present results for 136 levels with the GRASP code

GRASP2: Present results for 332 levels with the GRASP code

MCHF: Tayal (2008)

AS: Liang et al. (2010)

R: Ratio of velocity/length form of f- values from the GRASP1 calculations

4 LIFETIMES

The lifetime τ for a level j is defined as follows:

$$\tau_j = \frac{1}{\sum_i A_{ji}}. \quad (6)$$

Since this is a measurable parameter, it provides a check on the accuracy of the calculations. Therefore, in Table 1

we have listed our calculated lifetimes, which *include* the contributions from four types of transitions, i.e. E1, E2, M1 and M2.

In Table 4 we compare our lifetimes with the theoretical results of Gupta & Msezane (2005) from the CIV3 code (Hibbert 1975) and Froese-Fischer et al. (2006) from the MCHF code, plus the available measurements of Träbert et al. (1988, 1993), Pinnington et al. (1990), Moehs & Church

Table 4. Comparison of lifetimes (τ) for the lowest 40 levels of Fe XIV. All values are in ns *except* when specified under the column GRASP1.

Index	Configuration/Level	GRASP1	GRASP2	CIV3	MCHF	Experimental	
1	3s ² 3p	² P _{1/2} ^o	
2	3s ² 3p	² P _{3/2} ^o	16.93 ms	16.95	17.52±0.29a, 16.74±0.12b, 17.0±0.2c, 16.73 ^{+0.02} _{-0.01} d
3	3s3p ²	⁴ P _{1/2}	31.39	31.33	27.3898	27.53	29±3e
4	3s3p ²	⁴ P _{3/2}	167.5	166.4	153.0643	155.6	
5	3s3p ²	⁴ P _{5/2}	44.29	43.08	39.4166	40.14	39±5e
6	3s3p ²	² D _{3/2}	0.4145	0.4127	0.4209	0.3927	0.550±0.020, 0.460±0.050, 0.515±0.025, 0.340±0.060f
7	3s3p ²	² D _{5/2}	0.5269	0.5241	0.5414	0.5005	0.700±0.020, 0.630±0.025, 0.625±0.025, 0.530±0.040f
8	3s3p ²	² S _{1/2}	0.0510	0.0507	0.0531	0.0532	0.077±0.004, 0.054±0.004, 0.073±0.003, 0.061±0.006f
9	3s3p ²	² P _{1/2}	0.0267	0.0267	0.0280	0.0274	0.045±0.002, 0.045±0.003, 0.045±0.002, 0.035±0.007f
10	3s3p ²	² P _{3/2}	0.0229	0.0223	0.0243	0.0237	0.046±0.003, 0.030±0.003, 0.044±0.002, 0.034±0.007f
11	3s ² 3d	² D _{3/2}	0.0213	0.0215	0.0223	0.039±0.002, 0.038±0.002, 0.037±0.002, 0.032±0.006f
12	3s ² 3d	² D _{5/2}	0.0234	0.0236	0.0245	0.041±0.002, 0.040±0.002, 0.040±0.002, 0.032±0.005f
13	3p ³	² D _{3/2} ^o	0.2147	0.2204	0.2143	0.1915	
14	3p ³	² D _{5/2} ^o	0.2548	0.2614	0.2576	0.2392	
15	3p ³	⁴ S _{3/2} ^o	0.0271	0.0275	0.0287	0.0279	
16	3s3p(³ P)3d	⁴ F _{3/2} ^o	2.8721	2.902	0.4829	0.5013	1.5±0.2g
17	3s3p(³ P)3d	⁴ F _{5/2} ^o	3.1855	3.233	2.9590	3.229	1.9±0.1g
18	3p ³	² P _{1/2} ^o	0.0583	0.0593	0.0590	0.0593	
19	3p ³	² P _{3/2} ^o	0.0591	0.0602	0.0719	0.0739	
20	3s3p(³ P)3d	⁴ F _{7/2} ^o	3.547	3.606	3.3986	3.718	2.8±0.2g
21	3s3p(³ P)3d	⁴ F _{9/2} ^o	19.27 ms	19.29	
22	3s3p(³ P)3d	⁴ P _{5/2} ^o	0.0334	0.0335	0.0347	0.0336	
23	3s3p(³ P)3d	⁴ D _{3/2} ^o	0.0273	0.0275	0.0266	0.0275	
24	3s3p(³ P)3d	⁴ D _{1/2} ^o	0.0233	0.0235	0.0237	0.0237	
25	3s3p(³ P)3d	⁴ P _{1/2} ^o	0.0330	0.0331	0.0354	0.0342	
26	3s3p(³ P)3d	⁴ P _{3/2} ^o	0.0284	0.0285	0.0316	0.0296	
27	3s3p(³ P)3d	⁴ D _{7/2} ^o	0.0232	0.0234	0.0244	0.0238	
28	3s3p(³ P)3d	⁴ D _{5/2} ^o	0.0250	0.0252	0.0261	0.0258	
29	3s3p(³ P)3d	² D _{3/2} ^o	0.0263	0.0262	0.0274	0.0274	
30	3s3p(³ P)3d	² D _{5/2} ^o	0.0270	0.0269	0.0282	0.0283	
31	3s3p(³ P)3d	² F _{5/2} ^o	0.0552	0.0549	0.0575	0.0617	
32	3s3p(³ P)3d	² F _{7/2} ^o	0.0518	0.0516	0.0544	0.0585	
33	3s3p(³ P)3d	² P _{3/2} ^o	0.0182	0.0181	0.0185	0.0191	
34	3s3p(³ P)3d	² P _{1/2} ^o	0.0202	0.0201	0.0200	0.0211	
35	3s3p(¹ P)3d	² F _{7/2} ^o	0.0182	0.0181	0.0190	0.0329	
36	3s3p(¹ P)3d	² F _{5/2} ^o	0.0177	0.0176	0.0185	0.0323	
37	3s3p(¹ P)3d	² P _{1/2} ^o	0.0142	0.0144	0.0152	0.0273	
38	3s3p(¹ P)3d	² D _{3/2} ^o	0.0131	0.0134	0.0154	
39	3s3p(¹ P)3d	² P _{3/2} ^o	0.0134	0.0133	0.0127	0.0223	
40	3s3p(¹ P)3d	² D _{5/2} ^o	0.0118	0.0119	0.0122	0.0165	

GRASP1: present results with 136 levels from the GRASP code

GRASP2: present results with 332 levels from the GRASP code

CIV3: Gupta & Msezane (2005) from the CIV3 code

MCHF: Froese-Fischer et al. (2006)

a: Moehs & Church (1999)

b: Beiersdorfer et al. (2003)

c: Smith et al. (2005)

d: Brenner et al. (2007)

e: Träbert et al. (1988)

f: Pinnington et al. (1990), the first entry is for Free M-E Fit, the second for Constrained M-E Fit, the 3rd for VNET, and the 4th for ANDC

g: Träbert et al. (1993)

(1999), Beiersdorfer, Träbert & Pinnington (2003), Smith, Chutjian & Lozano (2005) and Brenner et al. (2007). In general, there are no discrepancies between the two calculations from GRASP and CIV3, or between theory and measurement. However, the differences for the $3s3p(^3P)3d^4F_{3/2}^o$ level (16) are particularly large. Our lifetime (2.90 ns) and that (2.11 ns) calculated by Träbert et al. (1993) are consistent, and comparable to the measured value (1.5 ns). However, the calculated lifetimes by Gupta & Msezane (2005) and Froese-Fischer et al. (2006), although agreeing with each other, are lower by up to a factor of 6. In fact, the *ab initio* calculation of Gupta & Msezane (2001) gives the lifetime of this level as 1.94 ns, but the use of their adjusted energies and subsequently the A- values lowers this value drastically.

5 COLLISION STRENGTHS

The *R*-matrix radius adopted for Fe XIV is 4.44 au, and 30 continuum orbitals have been included for each channel angular momentum in the expansion of the wave function. This large expansion is computationally more demanding as the corresponding size of the Hamiltonian matrix is 21,970. However, it permits us (without any loss of accuracy) to compute Ω up to an energy of 260 Ryd, i.e. about 250 Ryd *above* the highest threshold of Fe XIV considered in the work. This large range of energy allows us to calculate values of effective collision strength Υ (see section 6) up to $T_e = 1.2 \times 10^7$ K, well above the temperature of maximum abundance in ionisation equilibrium, i.e. 2.0×10^6 K (Bryans, Landi & Savin 2009). The maximum number of channels for a partial wave is 728 and all partial waves with angular momentum $J \leq 40$ are included. This large J range ensures convergence of Ω for all forbidden and inter-combination transitions, and at all energies. However, for some allowed transitions, particularly at higher energies, Ω are not fully converged within this range. We have therefore included a top-up, based on the Coulomb-Bethe approximation of Burgess & Sheorey (1974). Furthermore, we have included such contributions for forbidden transitions, based on geometric series, but these are small.

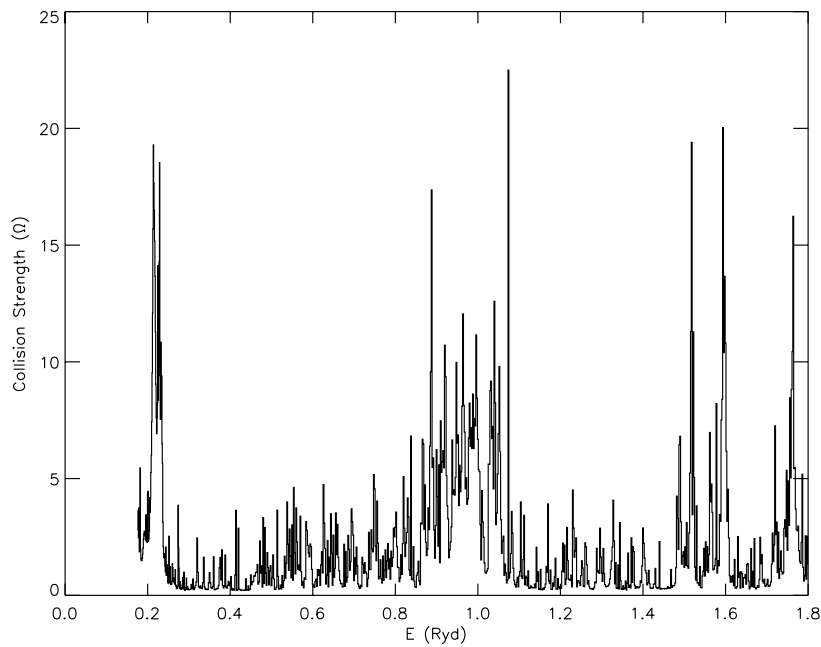
Storey et al. (2000) have reported values of Ω for some transitions from the ground state ($3s^23p^2P_{1/2,3/2}^o$) to higher excited levels, at an energy of 30 Ryd, and in Table 5 we compare our results with theirs. For the transitions listed in this table, most agree within 10%, except 2–3/4/5 (i.e. $3s^23p^2P_{3/2}^o - 3s3p^2^4P_{1/2,3/2,5/2}$) where there are differences of up to a factor of 2. These are inter-combination transitions and are forbidden in the *LS* coupling in which the calculations were (primarily) performed by Storey et al. Since no other results for Ω are available for comparison purposes, in Table 6 we list our Ω for all resonance transitions and at 6 energies above thresholds. These results will facilitate future comparisons and hence assessments of the accuracy of our data. However, based on comparisons of our calculations for other ions, such as Al X (Aggarwal & Keenan 2014a) and Si II (Aggarwal & Keenan 2014b), we assess the accuracy of our listed Ω to be better than 20% for most transitions of Fe XIV.

Table 5. Comparison of collision strengths (Ω) at an energy of 30 Ryd for some transitions of Fe XIV.

<i>i</i>	<i>j</i>	Present Results	Storey et al. (2000)
1	2	0.176
1	3	0.0171	0.0165
1	4	0.0064	0.0062
1	5	0.0050	0.0047
1	6	0.888	0.931
1	7	0.0142	0.0141
1	8	1.675	1.701
1	9	1.078	1.166
1	10	1.106	1.162
1	11	2.767	2.918
1	12	0.0281	0.0293
2	3	0.0050	0.0080
2	4	0.0056	0.0141
2	5	0.0299	0.0512
2	6	0.0556	0.0617
2	7	1.327	1.395
2	8	0.151	0.170
2	9	1.926	1.954
2	10	5.656	5.835
2	11	0.742	0.764
2	12	5.249	5.449

Table 6. Collision strengths for the resonance transitions of Fe XIV. ($a\pm b \equiv a \times 10^{\pm b}$). (For complete table see Supporting Information.)

Transition		Energy (Ryd)					
i	j	20	50	100	150	200	250
1	2	1.800-01	1.733-01	1.717-01	1.713-01	1.708-01	1.702-01
1	3	1.783-02	1.665-02	1.658-02	1.614-02	1.560-02	1.497-02
1	4	8.892-03	3.907-03	1.870-03	1.256-03	9.793-04	8.327-04
1	5	7.032-03	2.862-03	1.156-03	6.600-04	4.501-04	3.420-04
1	6	8.135-01	9.974-01	1.138-00	1.168-00	1.147-00	1.137-00
1	7	1.782-02	1.069-02	8.329-03	7.915-03	7.865-03	7.903-03
1	8	1.523-00	1.894-00	2.249-00	2.379-00	2.383-00	2.345-00
1	9	9.804-01	1.220-00	1.455-00	1.555-00	1.567-00	1.544-00
1	10	1.005-00	1.252-00	1.484-00	1.581-00	1.586-00	1.594-00
.
.
.


Figure 1. Collision strengths for the $3s^23p \ ^2P^{\circ}_{1/2} - 3s^23p \ ^2P^{\circ}_{3/2}$ (1-2) transition of Fe XIV.

6 EFFECTIVE COLLISION STRENGTHS

As already shown by Tayal (2008) and Liang et al. (2010), Ω does not vary smoothly within the thresholds region, especially for (semi) forbidden transitions. Such closed-channel (Feshbach) resonances need to be resolved in a fine energy mesh to accurately account for their contribution. In most astrophysical plasmas, electrons have a velocity distribution and therefore an averaged value, known as *effective* collision strength (Υ) is required. The most commonly used velocity distribution is *Maxwellian*, i.e.

$$\Upsilon(T_e) = \int_0^\infty \Omega(E) \exp(-E_j/kT_e) d(E_j/kT_e), \quad (7)$$

where k is Boltzmann's constant, T_e electron temperature in K, and E_j the electron energy with respect to the final (excited) state. Once the value of Υ is known the corresponding results for the excitation $q(i,j)$ and de-excitation $q(j,i)$ rates can be easily obtained from the following equations:

$$q(i, j) = \frac{8.63 \times 10^{-6}}{\omega_i T_e^{1/2}} \Upsilon \exp(-E_{ij}/kT_e) \quad \text{cm}^3 \text{s}^{-1} \quad (8)$$

and

$$q(j, i) = \frac{8.63 \times 10^{-6}}{\omega_j T_e^{1/2}} \Upsilon \quad \text{cm}^3 \text{s}^{-1}, \quad (9)$$

where ω_i and ω_j are the statistical weights of the initial (i) and final (j) states, respectively, and E_{ij} is the transition energy. The contribution of resonances may greatly enhance the values of Υ over those of the background collision strengths (Ω_B), but this depends strongly on the type of transition, and particularly the temperature. In general, the lower the T_e , the greater is the contribution of resonances. However, values of Ω need to be calculated over a wide energy range (above thresholds) to obtain convergence of the integral in Eq. (7), as demonstrated in fig. 7 of Aggarwal & Keenan (2008). For this reason we have calculated values of Ω up to an energy of 260 Ryd, as discussed in section 5 and hence in our work there is no need to invoke the high energy formulations of Burgess & Tully (1992), as undertaken by Liang et al. (2010).

To resolve resonances, we have calculated Ω in (most of) the thresholds region in a narrow energy mesh of 0.001 Ryd, although a mesh of 0.002 Ryd has also been used whenever the energy difference between any two thresholds is wider, such as levels 2 and 3. In total Ω have been calculated at over 10,500 energies, and in Figs. 1 – 3 we show resonance structure for three transitions, namely 1 – 2 ($3s^2 3p \ ^2P_{1/2}^o - 3s^2 3p \ ^2P_{3/2}^o$), 1 – 4 ($3s^2 3p \ ^2P_{1/2}^o - 3s 3p^2 \ ^4P_{3/2}$) and 1 – 6 ($3s^2 3p \ ^2P_{1/2}^o - 3s 3p^2 \ ^2D_{3/2}$), which are forbidden, inter-combination and allowed, respectively. Similar resonances in these transitions are also apparent from the data of Storey et al. (1996) and Tayal (2008) – see figs. 1–3 of the latter. For the important 1–2 transition, the magnitude of the resonances shown by Storey et al. (1996) are higher by almost a factor of 2, and this has also been noted by Liang et al. (2010) – see their fig. 3. As a consequence of this and some other factors, the Υ calculated by Storey et al. (1996) are significantly larger (by over a factor of 5), particularly towards the lower end of the temperature range, as demonstrated in fig. 4 of Tayal (2008). Resonances in our calculations for this transition are closer in magnitude to those of Tayal (2008),

but are comparatively greater in number. Similarly for the 1 – 4 transition, the resonance structure in our calculations is denser but their magnitude is more comparable to that of Tayal (2008) than of Storey et al. (1996). The density of resonances for the 1 – 6 transition is even more apparent in our work than that of Tayal (2008), although the peaks are narrow in width and hence may not make a significant contribution to Υ .

Our calculated values of Υ are listed in Table 7 over a wide temperature range up to $\log T_e = 7.1$ K, suitable for applications to a wide range of astrophysical plasmas. The inaccuracy of the Υ of Storey et al. (2000) has already been discussed and demonstrated by both Tayal (2008) and Liang et al. (2010), and therefore we make no comparison with their results. However, before we discuss any comparisons with the calculations of Tayal, we note that this is not straightforward, because his energy levels, A- values and Υ in tables 1, 3/4 and 5, respectively, have different orderings. The problem has partly arisen because his energy levels are neither in the NIST ordering nor in increasing energy, and mainly because he used different sets of wavefunctions for atomic structure (i.e. to determine energy levels and A-values) and the scattering process, i.e. to calculate Ω and Υ . Therefore, for undertaking a comparison with the Tayal data a careful (re)ordering is required for all his 135 levels, although his results for Υ are only provided up to level 59.

For the most important transition of Fe XIV, i.e. ($3s^2 3p \ ^2P_{1/2}^o - ^2P_{3/2}^o$ (1 – 2)), our results are shown in Fig. 4 along with those of Tayal (2008) and Liang et al. (2010). The Υ of Tayal are comparable to our calculations (within $\sim 20\%$), but those of Liang et al. are significantly higher (by up to a factor of two), particularly towards the lower end of the temperature range. In fact, at the lowest common temperature of $10^{3.593}$ K, the Υ of Liang et al. differ with our calculations by over 20% for $\sim 70\%$ of the transitions, and in a majority of cases their results are higher. For some transitions, such as 1 – 62/66/70/82/88/91/92/93, their data are greater by over an order of magnitude. Some differences between two calculations are understandable at low temperatures, because of the position of resonances, but not such large discrepancies as noted here. Similarly, at the highest common temperature of $10^{6.991}$ K, the discrepancies between our results and those of Liang et al. are over 20% for $\sim 46\%$ of the transitions, and as at lower temperatures their Υ values are higher for almost all transitions. Discrepancies of up a factor of 2 are common for many transitions, but are over an order of magnitude for some, such as 1 – 94/112/131, 2 – 94/132 and 3 – 83/106/122. The most likely reasons for such large discrepancies are those stated in section 1, but an error in the version of the code adopted by Liang et al. (2010) cannot be ruled out. Some versions of the *R*-matrix code are known to contain errors, particularly related to the Breit-Pauli part which accounts for the relativistic effects – see, for example, Aggarwal et al. (2000) who found large differences in *R*-matrix calculations for transitions in Fe XV, as did Aggarwal & Keenan (2012, 2013) more recently for Li-like ions. Another (strong) possibility is the presence of pseudo resonances, because in the generation of wave functions Liang et al. (2010) have included levels of additional 77 configurations which are not spectroscopic – see section 2. If the pseudo resonances are not properly smoothed over then the calculated values of Υ may be abnormally high. The

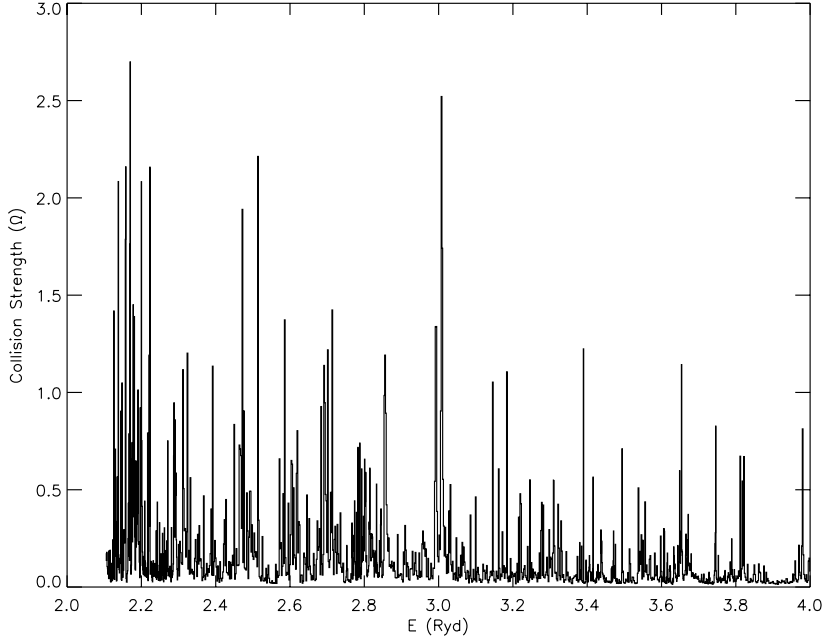


Figure 2. Collision strengths for the $3s^23p \ ^2P_{1/2}^\circ - 3s^23p \ ^2P_{1/2}^\circ - 3s3p^2 \ ^4P_{3/2}$ (1-4) transition of Fe XIV.

Table 7. Effective collision strengths for transitions in Fe XIV. ($a \pm b \equiv a \times 10^{\pm b}$). (For complete table see Supporting Information.)

Transition		Temperature (log T_e , K)							
i	j	5.70	5.90	6.10	6.30	6.50	6.70	6.90	7.10
1	2	1.643-00	1.344-00	1.055-00	8.065-01	6.115-01	4.677-01	3.660-01	2.925-01
1	3	6.773-02	5.311-02	4.181-02	3.358-02	2.783-02	2.392-02	2.118-02	1.886-02
1	4	9.967-02	7.390-02	5.375-02	3.868-02	2.764-02	1.964-02	1.387-02	9.712-03
1	5	1.059-01	7.747-02	5.553-02	3.929-02	2.755-02	1.916-02	1.322-02	9.024-03
1	6	1.487-00	1.323-00	1.181-00	1.080-00	1.025-00	1.011-00	1.019-00	1.010-00
1	7	2.148-01	1.633-01	1.221-01	8.988-02	6.542-02	4.739-02	3.446-02	2.524-02
1	8	1.287-00	1.307-00	1.350-00	1.420-00	1.519-00	1.643-00	1.770-00	1.834-00
1	9	8.417-01	8.575-01	8.903-01	9.398-01	1.003-00	1.080-00	1.158-00	1.197-00
1	10	8.847-01	8.952-01	9.201-01	9.621-01	1.023-00	1.102-00	1.186-00	1.229-00
.
.
.

ICFT results calculated by Liang et al. (2010) can sometimes significantly overestimate the values of Υ , in comparison to the corresponding Breit-Pauli work, at least for some of the transitions, as recently demonstrated and discussed by Storey, Sochi & Badnell (2014), see in particular their fig. 3. Finally, the Liang et al. data contain massive resonances for the 1 – 39 ($3s^23p \ ^2P_{1/2}^\circ - 3s3p(^1P)3d \ ^2P_{3/2}^\circ$) transition of Fe XIV (see their fig. 5) at energies below ~ 10 Ryd. However, our calculations do not show this, as may be seen from Fig. 5. As a result, the Υ of Liang et al. for this transition are

larger than the present calculations and those of Tayal by a factor of 2.

In Table 8, we compare our results of Υ with those of Liang et al. (2010) and Tayal (2008) for transitions among the lowest 10 levels of Fe XIV, at three common temperatures of 1.0×10^6 , 2.0×10^6 and 1.0×10^7 K. For these transitions at these temperatures, all sets of Υ (generally) agree within $\sim 20\%$, although the differences are slightly larger for a few, such as 2 – 6, 3 – 9/10 and 9 – 10. Such good agreement among three independent calculations is highly satisfactory

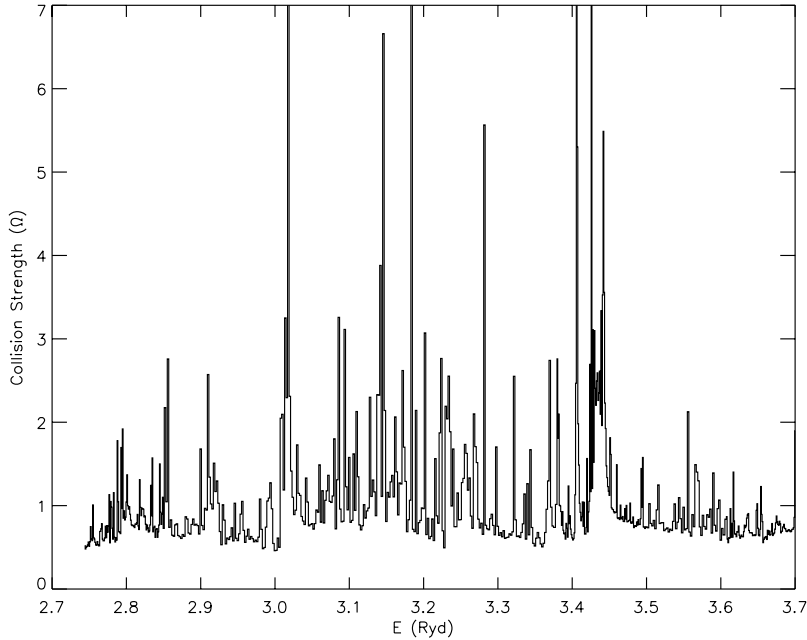


Figure 3. Collision strengths for the $3s^23p \ ^2P_{1/2}^\circ - 3s^23p \ ^2P_{1/2}^\circ - 3s3p^2 \ ^2D_{3/2}$ (1-6) transition of Fe XIV.

and encouraging, but is somewhat contrary to the discussion above. Furthermore, the most relevant temperature for Fe XIV is 2.0×10^6 K, that of maximum abundance in ionisation equilibrium (Bryans et al. 2009). At this T_e the discrepancies are less than 20% between our calculated Υ and those of Tayal (2008) for all transitions. However, this comparison is possible for only 630 transitions (i.e. $\sim 7\%$ of the total), because of the limited data reported by Tayal. Unfortunately, a similar comparison made at this T_e with the Υ of Liang et al. (2010) reveals that for about half the transitions there are differences of over 20%, and their results are mostly higher. Therefore, based on the comparisons shown in Table 8 and Fig. 4 and discussed above, we believe that the values of Υ calculated by Liang et al. are overestimated for almost all transitions and at all temperatures. Hence, a re-examination of their results is desirable.

7 CONCLUSIONS

In this paper we have presented results for energy levels and radiative rates for four types of transitions (E1, E2, M1 and M2) among the lowest 136 levels of Fe XIV. Additionally, lifetimes of all the levels have been reported, although measurements are available for only a few, for which there is good agreement between theory and experiment. Based on a variety of comparisons, our energy levels are assessed to be accurate to better than 1%, and the results for radiative rates, oscillator strengths, line strengths and lifetimes are

assessed to be accurate to better than 20% for a majority of the strong transitions (levels). Similarly, the accuracy of our data for collision strengths and effective collision strengths is estimated to be better than 20% for a majority of transitions. The earlier calculations of Liang et al. (2010) appear to have overestimated the values of Υ for almost all transitions and over an entire range of temperature. We believe the present set of results for radiative and excitation rates are the most complete and reliable to date, and hence should be useful for the modelling of a variety of plasmas. Finally, as Υ is a slowly varying function of T_e , corresponding data at any other temperature within the reported range can be easily interpolated, or may be requested from the first author.

ACKNOWLEDGMENTS

KMA is thankful to the Atomic Weapons Establishment, Aldermaston for financial support.

SUPPORTING INFORMATION

Additional Supporting Information may be found in the online version of this article:

Table 2. Transition wavelengths (λ_{ij} in Å), radiative rates (A_{ji} in s^{-1}), oscillator strengths (f_{ij} , dimensionless), and line strengths (S, in atomic units) for electric dipole (E1), and A_{ji} for E2, M1 and M2 transitions in Fe XIV. ($a \pm b \equiv a \times 10^{\pm b}$).

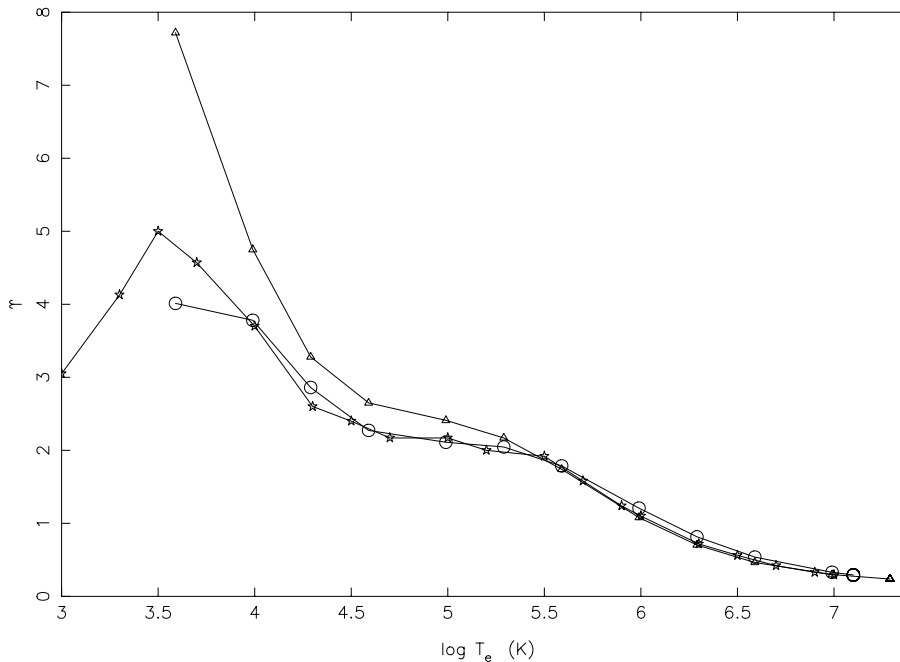


Figure 4. Comparison of effective collision strengths for the $3s^2 3p \ ^2P^o_{1/2} - 3s^2 3p \ ^2P^o_{3/2}$ (1– 2) transition of Fe XIV. Circles: present results, stars: Tayal (2008) and triangles: Liang et al. (2010).

Table 6. Collision strengths for the resonance transitions of Fe XIV. ($a \pm b \equiv a \times 10^{\pm b}$).

Table 7. Effective collision strengths for transitions in Fe XIV. ($a \pm b \equiv a \times 10^{\pm b}$).

REFERENCES

- Aggarwal K. M., Keenan F. P., 2012, *At. Data Nucl. Data Tables*, 98, 1003
- Aggarwal K. M., Keenan F. P., 2013, *At. Data Nucl. Data Tables*, 99, 156
- Aggarwal K. M., Keenan F. P., 2014a, *MNRAS*, 438, 1223
- Aggarwal K. M., Keenan F. P., 2014b, *MNRAS*, 442, 388
- Aggarwal K. M., Deb N. C., Keenan F. P., Msezane A. Z., 2000, *J. Phys. B*, 33, L391
- Aggarwal K. M., Keenan F. P., 2008, *Eur. Phys. J., D* 46, 205
- Aggarwal K. M., Tayal V., Gupta G. P., Keenan F. P., 2007, *At. Data Nucl. Data Tables*, 93, 615
- Badnell N. R., 1997, *J. Phys. B*, 30, 1
- Beiersdorfer P., Träbert E., Pinnington E. H., 2003, *ApJ*, 587, 836
- Berrington K. A., Burke P. G., LeDourneuf M., Robb W. D., Taylor K. T., Vo Ky Lan, 1978, *Comput. Phys. Commun.*, 14, 367
- Berrington K. A., Eissner W. B., Norrington P. H., 1995, *Comput. Phys. Commun.*, 92, 290
- Bhatia A. K., Kastner S. O., Keenan F. P., Conlon E. S., Widing K. G., 1994, *ApJ*, 427, 497
- Brenner G., Crespo López-Urrutia J. R., Harman Z., Mokler P. H., Ullrich J., 2007, *Phys. Rev., A* 75, 032504
- Brickhouse N. S., Raymond J. C., Smith B. W. 1995, *ApJS*, 97, 551
- Brosius J. W., Davila J. M., Thomas R. J., 1998, *ApJ*, 497, L113
- Brown C. M., Feldman U., Seely J. F., Korendyke C. M., Hara H., 2008, *ApJS*, 176, 511
- Bryans P., Landi E., Savin D. W., 2009, *ApJ*, 691, 1540
- Burgess A., Sheorey V. B., 1974, *J. Phys.*, B7, 2403
- Burgess A., Tully J. A., 1992, *A&A*, 254, 436
- Del Zanna G., Berrington K. A., Mason H.E., 2004, *Astron. Astrophys.* 422, 731
- Dermendjiev V. N., Kolarov G. V., Mitsev Ts. A., 1992, *Sol. Phys.*, 137, 199
- Dong C. Z., Kato T., Fritsche S., Koike F., 2006 *MNRAS*, 369, 1735
- Dufton P. L., Kingston A. E., 1991, *Phys. Scr.*, 43, 386
- Eissner W., Jones M., Nussbaumer H., 1974, *Comput. Phys. Commun.*, 8, 270
- Ferguson J. W., Korista K. T., Ferland G. J., 1997, *ApJS*, 110, 287
- Fisher R. R., 1978, *Sol. Phys.*, 57, 119
- Froese-Fischer C., 1991, *Comput. Phys. Commun.*, 64, 369
- Froese-Fischer C., Tachiev G., Irimia A., 2006, *At. Data Nucl. Data Tables*, 92, 607

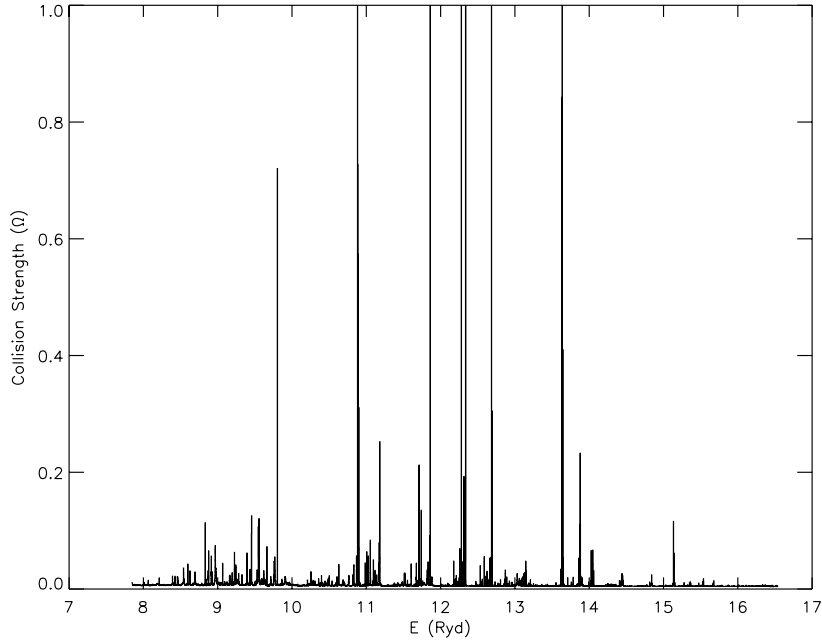


Figure 5. Collision strengths for the $3s^2 3p \ ^2P^{\circ}_{1/2} - 3s 3p(^1P) 3d \ ^2P^{\circ}_{3/2}$ (1– 39) transition of Fe XIV.

- Grant I. P., McKenzie B. J., Norrington P. H., Mayers D. F., Pyper N. C., 1980, *Comput. Phys. Commun.*, 21, 207
- Gupta G. P., Msezane A. Z., 2001, *J. Phys. B* 34, 4217
- Gupta G. P., Msezane A. Z., 2005, *At. Data Nucl. Data Tables*, 89, 1
- Hibbert A., 1975, *Comput. Phys. Commun.*, 9, 141
- Hibbert A., 2000, *AIP Conf. Proc.*, 543, 242
- Huang K. N., 1989, *At. Data Nucl. Data Tables*, 34, 1
- Jupén C., Isler R. C., Träbert E., 1993, *MNRAS*, 264, 627
- Kramida A., Ralchenko Y., Reader J. and NIST ASD Team, 2013, *NIST Atomic Spectra Database (version 5.1)* Online at: <http://physics.nist.gov/asd>
- Lamzin S. A., Stempels H. C., Piskunov N. E., 2001, *A&A*, 369, 965
- Liang G. Y., Badnell N. R., Crespo López-Urrutia J. R., Baumann T. M., Del Zanna G., Storey P. J., Tawara H., Ullrich J., 2010, *ApJS*, 190, 322
- Moehs D. P., Church D. A., 1999, *ApJ*, 516, L111
- Pinnington E. H., Ansbacher W., Tauheed T., Träbert E., Heckmann P. H., Möller G., Blanke J. H., 1990, *Z. Phys. D* 17, 5
- Safronova U. I., Sataka M., Albritton J. R., Johnson W. R., Safronova M. S., 2002, *Phys. Rev. A*, 65, 022507
- Smith S. J., Chutjian A., Lozano J. A., 2005, *Phys. Rev. A* 72, 062504
- Storey P. J., Mason H. E., Saraph H. E., 1996, *A&A*, 309, 677
- Storey P. J., Mason H. E., Young P. R., 2000, *A&AS*, 141, 285
- Storey P. J., Sochi T., Badnell N. R., 2014, *MNRAS*, 441, 3028
- Tayal S. S., 2008, *ApJS*, 178, 359
- Thomas R. J., Neupert W. M., 1994, *ApJS*, 91, 461
- Träbert E., Heckmann P. H., Hutton R., Martinson I., 1988, *J. Opt. Soc. Am. B* 5, 2173
- Träbert E., Wagner C., Heckmann P. H., Möller G., Brage T., 1993, *Phys. Scr.*, 48, 593
- Wei H. L., Zhang H., Ma C. W., Zhang J. Y., Cheng X. L., 2008, *Phys. Scr.*, 77, 035301
- Young P. R., Landi E., Thomas R. J., 1998, *A&A*, 329, 291
- Zatsarinny O., Froese-Fischer C., 1999, *Comput. Phys. Commun.*, 124, 247

Table 8. Comparison of effective collision strengths (Υ) at three temperatures for transitions among the lowest 10 levels of Fe XIV. $a \pm b \equiv a \times 10^{\pm b}$.

Transition		Present Results			Liang et al. (2010)			Tayal (2008)		
i	j	1.0×10^6 K	2.0×10^6 K	1.0×10^7 K	1.0×10^6 K	2.0×10^6 K	1.0×10^7 K	1.0×10^6 K	2.0×10^6 K	1.0×10^7 K
1	2	1.209-0	8.065-1	3.299-1	1.08-0	7.04-1	2.98-1	1.10+0	7.18-1	2.94-1
1	3	4.755-2	3.358-2	2.012-2	4.87-2	3.47-2	2.06-2	5.50-2	3.70-2	2.00-2
1	4	6.403-2	3.868-2	1.180-2	6.29-2	3.99-2	1.25-2	6.70-2	4.10-2	1.20-2
1	5	6.669-2	3.929-2	1.112-2	7.18-2	4.40-2	1.25-2	6.90-2	4.10-2	1.10-2
1	6	1.254-0	1.080-0	1.020-0	8.37-1	8.41-1	1.02-0	7.91-1	7.90-1	9.65-1
1	7	1.433-1	8.988-2	2.988-2	1.34-1	8.43-2	2.82-2	1.31-1	8.10-2	2.60-2
1	8	1.323-0	1.420-0	1.813-0	1.30-0	1.40-0	1.84-0	1.25+0	1.33+0	1.77+0
1	9	8.702-1	9.398-1	1.184-0	8.87-1	9.52-1	1.25-0	1.00+0	1.06+0	1.35+0
1	10	9.046-1	9.621-1	1.215-0	9.15-1	9.68-1	1.25-0	9.44-1	9.82-1	1.23+0
2	3	5.133-2	3.062-2	1.149-2	5.17-2	3.29-2	1.39-2	5.70-2	3.50-2	1.40-2
2	4	1.115-1	6.569-2	2.049-2	1.10-1	6.99-2	2.58-2	1.22-1	7.40-2	2.50-2
2	5	1.990-1	1.273-1	5.698-2	1.97-1	1.36-1	7.13-2	2.03-1	1.33-1	6.50-2
2	6	3.140-1	2.081-1	9.169-2	2.33-1	1.61-1	8.77-2	2.22-1	1.50-1	8.30-2
2	7	1.441-0	1.363-0	1.448-0	1.42-0	1.37-0	1.57-0	1.31+0	1.26+0	1.51+0
2	8	1.717-1	1.582-1	1.679-1	1.98-1	1.85-1	2.04-1	2.31-1	2.17-1	2.54-1
2	9	1.536-0	1.644-0	2.078-0	1.55-0	1.65-0	2.16-0	1.54+0	1.62+0	2.11+0
2	10	4.496-0	4.828-0	6.144-0	4.52-0	4.85-0	6.36-0	4.63+0	4.90+0	6.29+0
3	4	4.055-1	2.514-1	8.283-2	4.59-1	2.92-1	9.37-2	4.21-1	2.64-1	8.50-2
3	5	3.796-1	2.959-1	2.105-1	4.68-1	3.55-1	2.28-1	3.96-1	3.10-1	2.12-1
3	6	9.266-2	5.558-2	1.675-2	8.80-2	5.62-2	1.71-2	8.30-2	5.20-2	1.60-2
3	7	6.618-2	3.818-2	9.992-3	6.94-2	4.27-2	1.13-2	6.60-2	4.00-2	1.10-2
3	8	3.067-2	1.747-2	4.315-3	3.94-2	2.36-2	5.89-3	3.40-2	2.10-2	5.00-3
3	9	2.157-2	1.177-2	2.668-3	3.01-2	1.77-2	4.35-3	5.00-2	2.70-2	6.00-3
3	10	3.244-2	1.814-2	4.598-3	4.37-2	2.55-2	6.29-3	3.70-2	2.20-2	5.00-3
4	5	1.604-0	1.067-0	4.548-1	1.35-0	9.15-1	4.19-1	1.26+0	8.59-1	4.02-1
4	6	1.588-1	9.461-2	2.572-2	1.36-1	8.63-2	2.46-2	1.32-1	8.20-2	2.50-2
4	7	2.740-1	1.614-1	4.662-2	2.13-1	1.34-1	4.12-2	2.10-1	1.31-1	4.00-2
4	8	5.016-2	2.854-2	7.051-3	5.16-2	3.14-2	8.06-3	5.20-2	3.20-2	8.00-3
4	9	4.891-2	2.707-2	6.688-3	4.70-2	2.81-2	7.31-3	4.80-2	2.80-2	7.00-3
4	10	1.001-1	5.503-2	1.312-2	9.85-2	5.76-2	1.44-2	9.90-2	5.80-2	1.50-2
5	6	1.524-1	9.259-2	2.915-2	1.52-1	9.72-2	3.07-2	1.39-1	8.80-2	2.70-2
5	7	3.491-1	2.211-1	8.114-2	3.80-1	2.48-1	8.76-2	3.19-1	2.11-1	7.30-2
5	8	5.292-2	3.169-2	9.999-3	6.16-2	3.82-2	1.09-2	5.50-2	3.40-2	1.00-2
5	9	5.833-2	3.418-2	1.012-2	5.28-2	3.25-2	9.08-3	5.20-2	3.20-2	9.00-3
5	10	1.307-1	7.161-2	1.683-2	1.40-1	8.31-2	2.10-2	1.33-1	7.90-2	2.00-2
6	7	9.828-1	6.233-1	2.586-1	9.64-1	6.20-1	2.60-1	9.00-1	5.82-1	2.43-1
6	8	2.869-1	2.353-1	1.885-1	2.90-1	2.42-1	1.96-1	2.93-1	2.50-1	2.05-1
6	9	2.639-1	1.705-1	8.318-2	2.51-1	1.66-1	8.03-2	2.50-1	1.64-1	7.59-2
6	10	2.587-1	1.539-1	5.095-2	2.65-1	1.62-1	5.24-2	2.61-1	1.59-1	5.27-2
7	8	4.262-1	3.665-1	3.128-1	4.31-1	3.74-1	3.21-1	4.41-1	3.88-1	3.44-1
7	9	1.592-1	1.138-1	6.808-2	1.62-1	1.18-1	6.89-2	1.51-1	1.09-1	5.66-2
7	10	4.992-1	2.802-1	7.187-2	4.74-1	2.76-1	7.14-2	4.36-1	2.54-1	6.79-2
8	9	2.385-1	1.377-1	3.462-2	2.82-1	1.66-1	4.17-2	2.75-1	1.64-1	4.11-2
8	10	3.933-1	2.325-1	7.232-2	4.48-1	2.65-1	7.67-2	4.12-1	2.44-1	7.00-2
9	10	3.550-1	2.563-1	1.541-1	5.02-1	3.48-1	1.81-1	3.70-1	2.71-1	1.66-1